USGS Earthquake Hazards Program Final Technical Report for External Research Support

USGS Award Number: G14AP00072

Title of Award: Long term slip rate along the Banning strand of the southern San Andreas Fault at Devers Hill

Principle Investigator: Whitney M. Behr, Dept. of Geological Sciences, Jackson School of Geosciences, University of Texas Austin.
2275 Speedway Stop C9000, Austin, TX, USA 78712-1722

Term covered: July 1, 2014 – July 1, 2015

Abstract

Northwest directed slip from the southern San Andreas Fault is transferred to the Mission Creek, Banning, and Garnet Hill fault strands in the northwestern Coachella Valley. How slip is partitioned between these three faults is critical to southern California seismic hazard estimates, but is poorly understood. The goal of this project, funded by the USGS Earthquake Hazards Program and the Southern California Earthquake Center (SCEC), was to fill one major outstanding data gap by measuring the slip rate of the Banning strand of the southern San Andreas Fault. In this Final Technical Report, we describe the primary result of this project: the first slip rate measured for the Banning fault strand. We constrain the depositional age of an alluvial fan offset 25 ± 5 m from its source by the Banning strand to between 5.1 ± 0.4 ka (95% C.I.) and 6.4 +3.7/-2.1 ka (95% C.I.) using U-series dating of pedogenic carbonate clast-coatings and ^{10}Be cosmogenic nuclide exposure dating of surface clasts. We calculate a Holocene geologic slip rate for the Banning strand of 3.9 +2.3/-1.6 mm/yr (median, 95% C.I.) to 4.9 +1.0/-0.9 mm/yr (median, 95% C.I.). This rate represents only 25-35% of the total slip accommodated by this section of the southern San Andreas Fault, suggesting a model in which slip is less concentrated on the Banning strand than previously thought. In rejecting the possibility that the Banning strand is the dominant structure, our results highlight an even greater need for slip rate and paleoseismic measurements along faults in the northwestern Coachella Valley in order to test the validity of current earthquake hazard models. In addition, our comparison of ages measured with U-series and ^{10}Be exposure dating demonstrates the importance of using multiple geochronometers when estimating the depositional age of alluvial landforms.

Report

The following summarizes results reported in the recent article "Holocene geologic slip rate of the Banning Strand of the southern San Andreas Fault, southern California", published in the *Journal of Geophysical Research* by authors Gold, Behr, Rood, Sharp, Rockwell, Kendrick and Salin. A PDF of this paper is included at the end of this report.

1. Introduction

The Coachella Valley segment of the southern San Andreas Fault in southern California consists of a system of faults that increase in complexity toward the northwest, from a single right-lateral strand at Bombay Beach (Indio strand), to an intricate network of right-lateral-reverse faults in the San Gorgonio Pass region (Allen, 1957; Matti and Morton, 1993) (Fig. 1). Because the Coachella Valley segment is considered well past its average earthquake recurrence interval (Fumal et al., 2002; Fialko, 2006; Weldon et al., 2005; Field et al., 2009; Philibosian et al., 2011), an understanding of how these faults interact to accommodate Pacific-North American plate motion and transfer slip to other faults within the San Andreas Fault System is critical to realistically assessing seismic hazard and, more broadly, to understanding the evolution of long-lived strike-slip fault systems over different spatial and temporal scales.

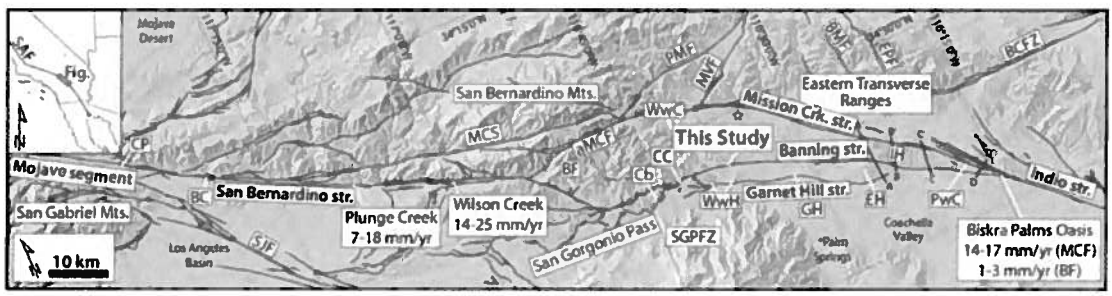

Figure 1 Fault map of the southern San Andreas Fault (SAF) system in the vicinity of San Gorgonio Pass. Late Quaternary fault slip rates have been determined at Plunge Creek (McGill et al., 2013) and Wilson Creek (Harden and Matti, 1989) along the San Bernardino strand and at Biskra Palms Oasis (Behr et al., 2010; Van der Woerd et al., 2006; Keller et al., 1982) along the Coachella Valley segment, of which the Banning, Mission Creek, Garnet Hill and Indio strands are a part. This study contributes the first slip rate for the Banning strand (Banning str.) at its northwest end. Cross-sections A-D illustrating structural deformation within the Indio Hills are presented in Figure 5. Star north of study area indicates the epicenter of the 1986 M5.9 North Palm Springs. aMCF – ancestral Mission Creek Fault; BC – Badger Canyon; BCFZ – Blue Cut Fault zone; BF – Burro Flats; BMF – Burnt Mountain Fault; Cb – Cabazon; CC – Cottonwood Canyon; CP – Cajon Pass; EH – Edom Hill; EPF – Eureka Peak Fault; GH – Garnet Hill; IH – Indio Hills; MCS – Mission Creek strand; MVF – Morongo Valley Fault; PMF – Pinto Mountain Fault; PwC – Pushwalla Canyon; SGPFZ – San Gorgonio Pass Fault Zone; SJF – San Jacinto Fault; WwC – Whitewater Canyon; WwH – Whitewater Hills.

At Biskra Palms Oasis in the southeastern Indio Hills (Fig. 1), about 50 km southeast of San Gorgonio Pass (Van der Woerd et al., 2006; Behr et al., 2010; Keller et al., 1982), the Indio strand of the Coachella Valley segment splits into three additional primary strands: the Mission Creek, Banning and Garnet Hill strands. The slip rate on the Mission Creek strand of the fault is 12-22 mm/yr averaged over ~50 ky, but how slip is partitioned between the primary structures (Banning, Mission Creek and Garnet Hill strands) to the northwest is entirely unconstrained. In this study, we investigate this issue by 1) presenting new geomorphic and structural constraints on fault kinematics and slip transfer between the Banning and Mission Creek strands within the Indio Hills and 2) providing the first quantitative estimate of the slip rate for the Banning strand in the northwestern Coachella Valley. We discuss the implications of these new data for seismic hazard and slip partitioning in southern California.

2. Tectonic Setting

As described in Gold et al (2015), geologic slip rates measured to the north and south of San Gorgonio Pass permit interpretations wherein ~50 to 100% of the total slip from the Coachella Valley segment is transferred northwest to the San Bernardino strand. There is little evidence for significant latest Quaternary slip on the ancestral Mission Creek Fault or the Mill Creek strand in the San Bernardino Mountains (Matti et al., 1992; Weldon, 2010; Sieh, 1994; Kendrick et al., 2015). Thus, slip transfer from the southern Mission Creek strand to the Banning and Garnet Hill strands and eventually to the San Gorgonio Pass Fault zone must be the primary mechanism by which slip, regardless of the amount, propagates northwest from the Coachella Valley segment to the San Bernardino strand. In the absence of quantitative slip rate data, two end member rupture scenarios for an earthquake that nucleates on the Indio strand of the Coachella Valley segment may be possible:

1) Rupture may propagate northwest primarily along the Banning strand (Fig. 2a), transferring slip into the San Gorgonio Pass Fault zone and potentially threatening southern California populations, as is considered probable by the UCERF 3 hazard model (Field et al., 2014; 2015);

2) Rupture may propagate northwest primarily along the Mission Creek strand (Fig. 2b) and transfer slip away from southern California populations via faults in the Eastern Transverse Ranges.

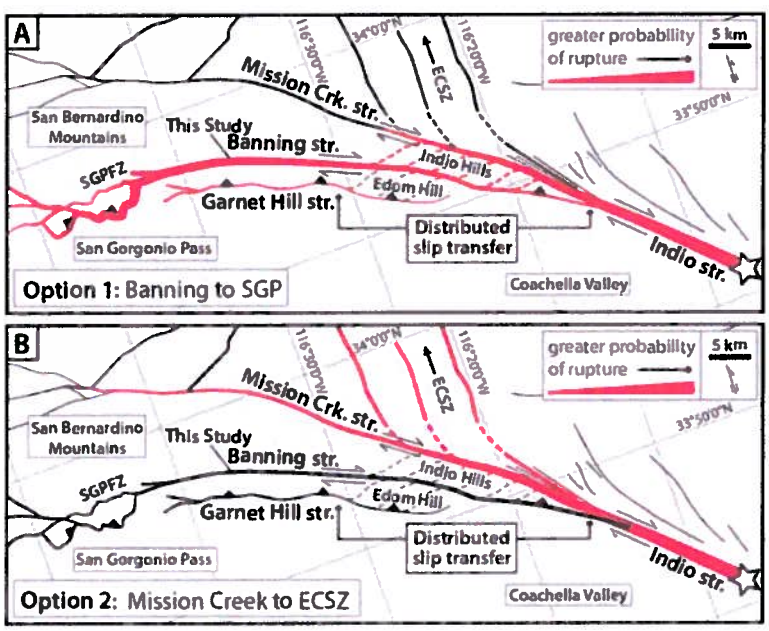

Figure 2 End member options for slip partitioning and the probable distribution of displacement on the Mission Creek, Banning and Garnet Hill strands during a future rupture on the Coachella Valley segment of the southern San Andreas Fault. A) Option1: Future ruptures are most likely to follow the Banning strand. This option is consistent with a fast (≥15 mm/yr) slip rate at the study location. B) Option 2: Future

ruptures are equally likely to bypass the Banning strand in favor of the Mission Creek strand and eventual transfer of slip to the Eastern California Shear Zone. This option is consistent with a slow (<10 mm/yr) slip rate at our study site. Intermediate scenarios are also possible, including rupture of the Garnet Hill strand with the Banning strand and a more even distribution of slip between all three faults. Distinguishing between these models requires slip rate data for the Banning strand.

More evenly distributed slip partitioning and multi-path rupture scenarios, including slip on the Garnet Hill strand, that lie between these two end-members are also possible. In subsequent sections we will discuss both qualitative and quantitative constraints on the minimum slip transfer that occurs between these two important fault strands in the northern Coachella Valley, focusing primarily on the geomorphology, structure and slip rate on the Banning strand.

3. Geomorphic and structural evidence of slip transfer

We used the B4 LiDAR data, Google Earth imagery, and field observations to systematically investigate the tectonic geomorphology of the Banning and Mission Creek strands in the northern Coachella Valley (Fig. 3). The gradients in surface expression observed along strike of the Banning and Mission Creek strands and the geomorphic and erosional changes in the Indio Hills are consistent with a model in which slip transfers from Mission Creek strand to the Banning strand in the northwestern Indio Hills.

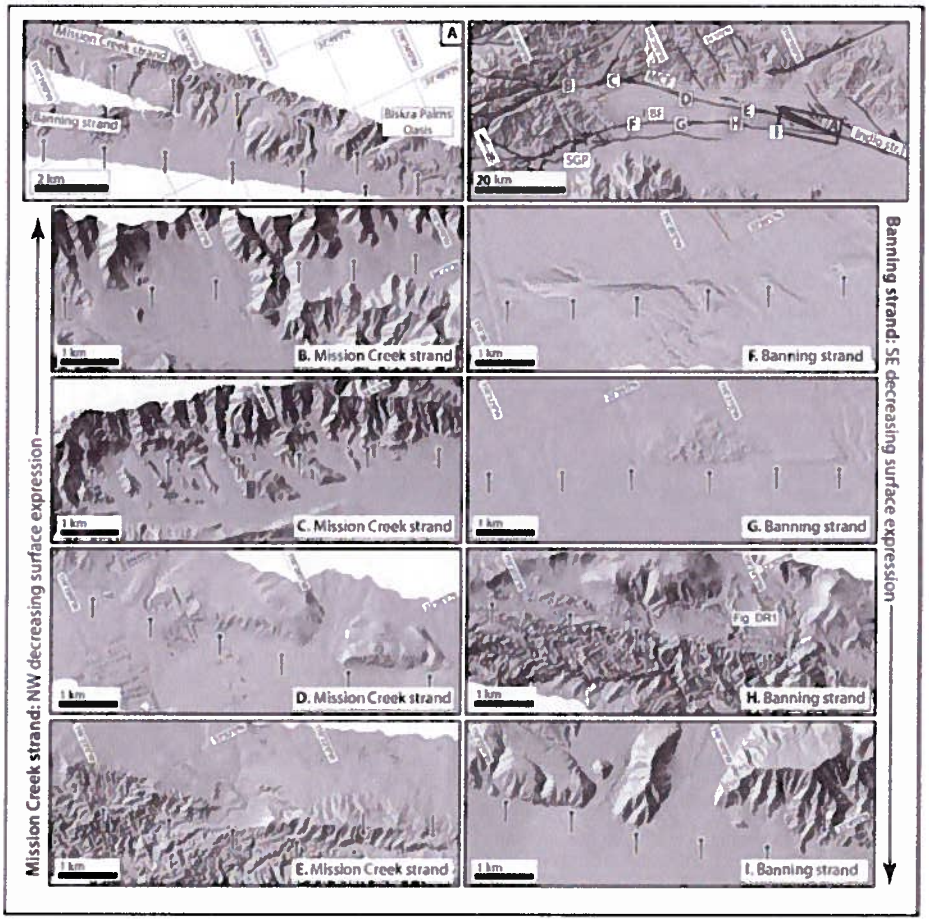

Figure 3 Shaded relief images showing geomorphic evidence of active faulting along sections of the Mission Creek (B-E) and the Banning strand (F-I) from their junction at the south end of the Indio Hills (A) to the San Bernardino Mountains and San Gorgonio Pass to the northwest. Images are derived from B4 airborne LiDAR; black and white arrows indicate the fault surface traces as observed or inferred by lidar-based observations. Figure locations along each fault are shown on the upper-right map. Upper-right abbreviations: San Gorgonio Pass (SGP), Mission Creek fault strand (MCF), Banning fault strand (BF), Coachella Valley segment of the southern San Andreas Fault (CV-SAF). The northwest-increasing geomorphic expression of the Banning strand is coincident with the northwest-decrease in geomorphic expression of the Mission Creek strand, suggesting that the Banning strand is the most active structure by the time both faults exit the Coachella Valley.

We also constructed new cross sections illustrating the internal structure of the Indio Hills (Fig. 4) by combining existing structural data and geologic mapping (Dibblee, 2008) with new structural measurements collected along major N-S trending channels that cross the Indio Hills. Along-strike variations in fault dip and deformation patterns indicate that significant slip transfer occurs between the Mission Creek and Banning strands, and between the Banning and Garnet Hill strands over both long (Quaternary) and short (Holocene) timescales. Both the geomorphic and structural observations and measurements collected during this study are described in greater detail in Gold et al. (2015).

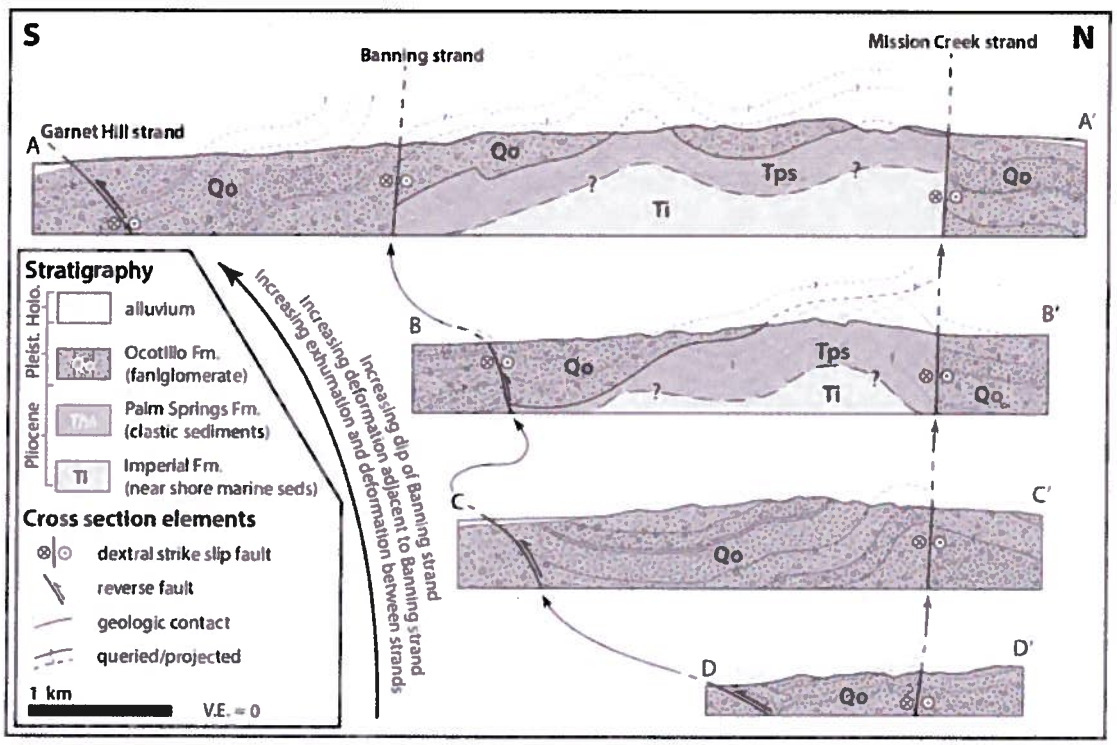

Figure 4 Cross sections traversing the Indio Hills based on structural mapping showing along-strike gradients in fault dip and deformation of the Ocotillo and Palm Springs Formations between the Banning, Mission Creek and Garnet Hill strands. The northwest increase in exhumation, folding and topography between the two faults and the increasing dip of the Banning strand provides structural evidence for the transfer of right lateral slip from the Mission Creek strand to the Banning strand within the Indio Hills. The greater deformation adjacent to the Banning strand shown at the SW edge of A-A' suggests subsequent transfer of some displacement to the Garnet Hill strand.

4. Geologic slip rate for the Banning Strand

The geomorphologic and structural data discussed in previous sections suggests significant slip transfer between the Mission Creek and Banning strands, but does not provide quantitative information as to *how much* slip is concentrated on the Banning strand as it enters San Gorgonio Pass. To investigate this, we use offset measurements and Quaternary geochronology to estimate the slip rate at a newly identified site along the Banning strand near the eastern entrance to San Gorgonio Pass, which we informally refer to as the "Painted Hill" site.

In the southeastern section of San Gorgonio Pass, the 285° trending, steeply dipping Banning strand separates moderately SE-dipping Pliocene fanglomerates north of the fault from beheaded late Pleistocene and Holocene alluvial fans south of the fault. At this location (33.942005° N, -116.620846° E), the Banning strand offsets a small alluvial fan, which we refer to as Qfr, from its small (~0.03 km^2) source catchment north of the fault (Fig. 5). Previous mapping did not differentiate this small (also ~0.03 km^2 in area) deposit from an older, truncated and tilted alluvial fan surface (Qoa3s on Figure 5), which it overlies.

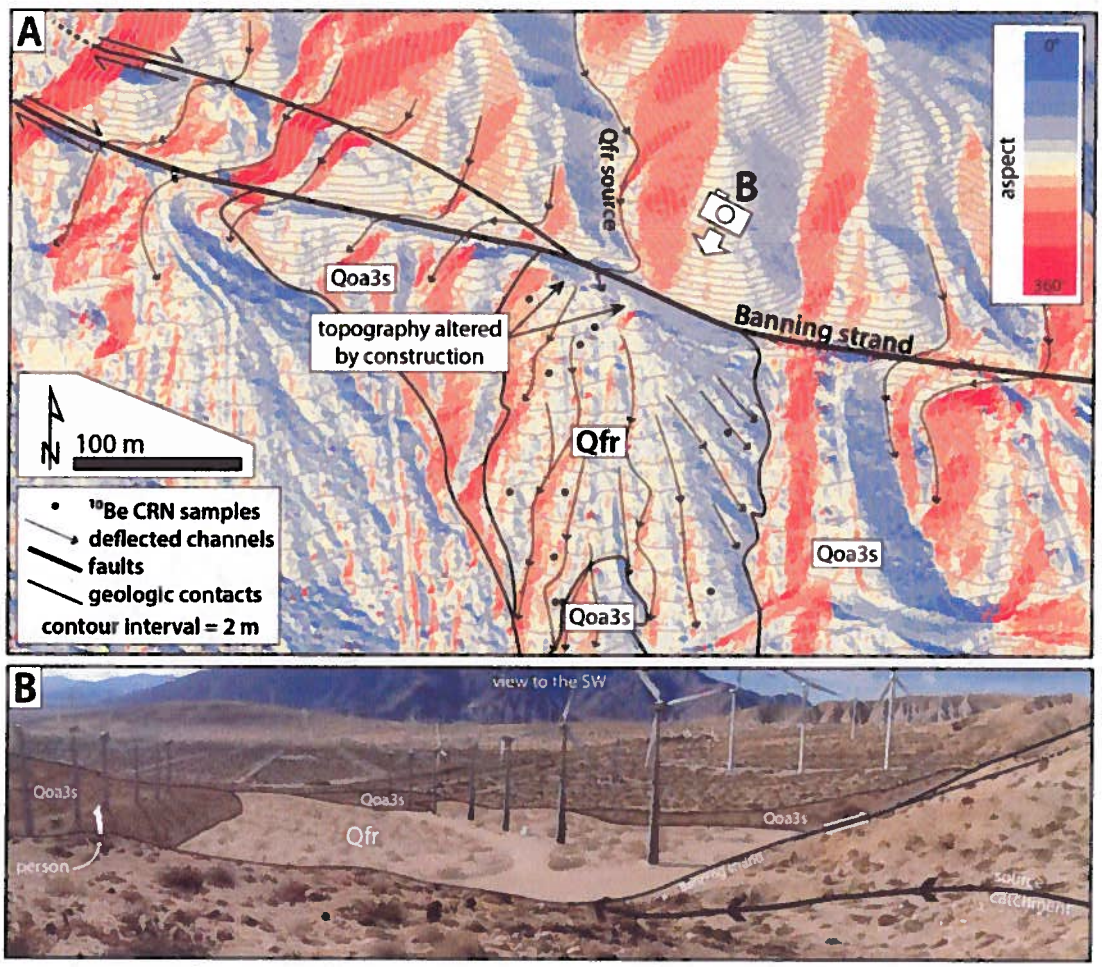

Figure 5 Aspect colored slope shade map of the offset Qfr alluvial fan (A), which was deposited on top of the older Qoa3s alluvial deposit during no more than 2 debris flow events. 2 m contours reveal typical alluvial fan curvature. Black dots show sampling locations for U-series and ^{10}Be exposure dating. Offset

and deflected to the east and west signify predominantly right lateral slip along this section of the Banning strand. Topography and fan morphology near the top of Qfr are have been disrupted by construction. B. Annotated panoramic photograph of the field site looking to the southwest from the vantage shown in A.

To quantitatively locate the axis of Qfr and determine by how much it has been laterally displaced, we designed a novel Matlab-based method that approximates the fan curvature by fitting circles extracted contours lines (Fig. 6). This calculation results in two nearly identical distributions of circle centers from both linear and non-linear fits. Since circles are not forced to be concentric using this method, the circle centers define linear distributions that we interpret to reflect the location and azimuth of the fan axis because they match the location and orientation of both the topographic drainage divide and the fan axis determined visually from the aspect map of the Qfr fan (Fig. 5a). As a last step we calculated a linear least squares fit through both groups of circle centers to provide a linear approximation of the axis. A detailed description of the workflow, the Matlab code and a link to the fitcircle download page are provided in the Supporting Information of Gold et al. (2015). Using this method we find that the fan axis, which should extend away from the mouth of the modern catchment, is offset from the modern catchment thalweg by 25 ± 5 m (min-preferred-max) in a direction parallel to fault strike (Fig. 7).

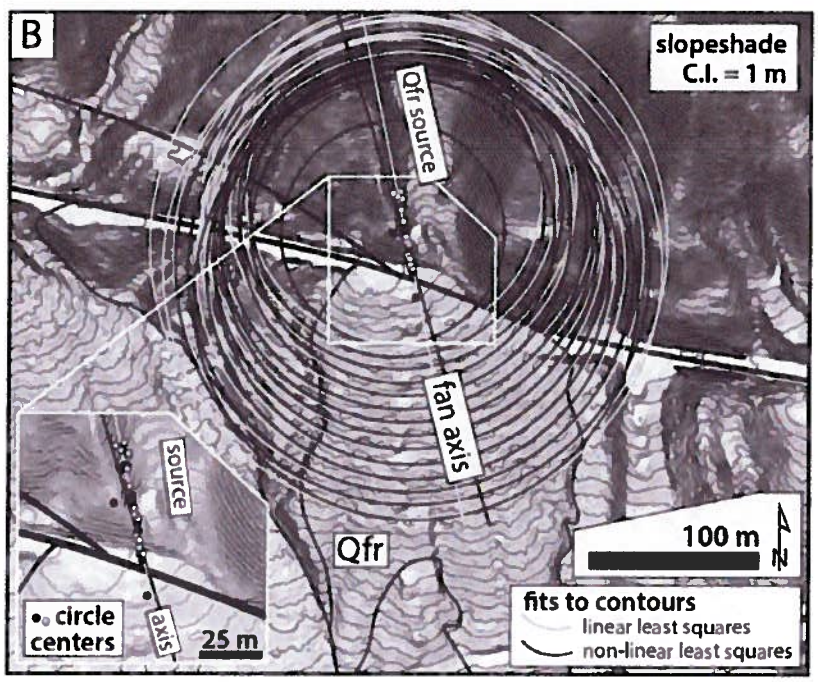

Figure 6 Topography-based method for approximating the axis of the Qfr fan. The upper four contours reflect topography modified by construction and are excluded from the analysis. Linear and non-linear least squares circle fits to the contours result in linear distributions of the circle centers that approximate the orientation and along strike location of the fan axis. The quantitatively constrained fan axis serves as the offset piercing line, which we reconstruct ~25 m the Qfr source catchment.

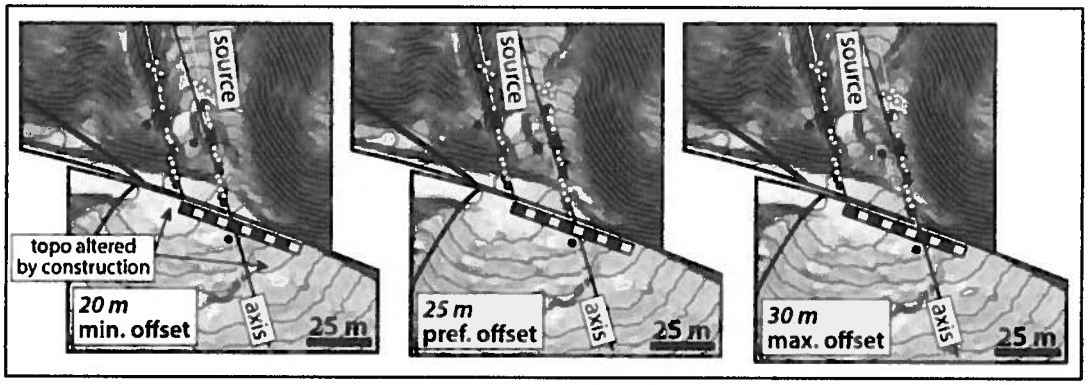

Figure 7 Minimum (A), preferred (B) and maximum (C) offsets measured by reconstructing the axis of the Qfr fan to the mouth of its source catchment indicate between 20 and 30 m of right lateral displacement since deposition. The scale bar along the fault represents 50 m; increments are 5 m. The offset error of 5 m reflects uncertainty in the location of the catchment thalweg at the time of deposition.

To constrain the depositional age of the Qfr fan we used both cosmogenic exposure dating and U-series dating of pedogenic carbonate. Exposure ages from 2 small boulders, 7 cobbles, and a selection of amalgamated pebbles range from 2.4 ka to 9.2 ka (not corrected for inheritance) with individual 2σ total uncertainties of around ±20%. We use probability distributions to model a composite exposure age for the clasts collected from the Qfr alluvial fan (Zechar and Frankel, 2009). Combining ^{10}Be exposure ages from surface clasts and using total uncertainties and assuming a Gaussian distribution of individual ages yields a median composite exposure age of 6.4 +3.7/-2.1 ka (95% C.I.). The exclusion of two clast samples from the final age is discussed at length in Gold et al. (2015). Modeling the depth profile data (7 depth intervals) using the Monte Carlo simulator presented in Hidy et al. (2010) gives an inheritance corrected age of 2.9 ± 0.70 ka (2σ), and indicates 1.56-2.0 x10^4 atoms/g inherited ^{10}Be, which is equivalent to 3.0 ± 0.25 kyr (1σ internal uncertainty) of prior exposure.

All of the U-series ages agree within uncertainties. We note that scatter of the U-series ages beyond that expected from analytical uncertainties is absent, consistent with closed U-Th systems and the absence of inherited clast-coatings. Three relatively precise analyses (those with the smallest corrections for ^{230}Th from detritus) with ages of 4.70 ± 0.92 ka (2σ), 4.87 ± 0.84 ka and 5.40 ± 0.72 ka are in good mutual agreement. Because the youngest dates are likely to be those biased most by relatively late growth of their clast-coatings, we adopt the weighted mean age of the eight remaining samples, 5.09 ± 0.44 (95% C.I.; MSWD = 0.57), as our best estimate of the minimum age of the Qfr fan. We emphasize that this measurement simply constrains Qfr deposition to no later than ~5 ka. because the median clast exposure age and U-series carbonate age agree satisfactorily, we favor these ages and not the depth profile age for the slip rate calculation. Exposure age and U-series data used to calculate the slip rates are shown in Figure 8.

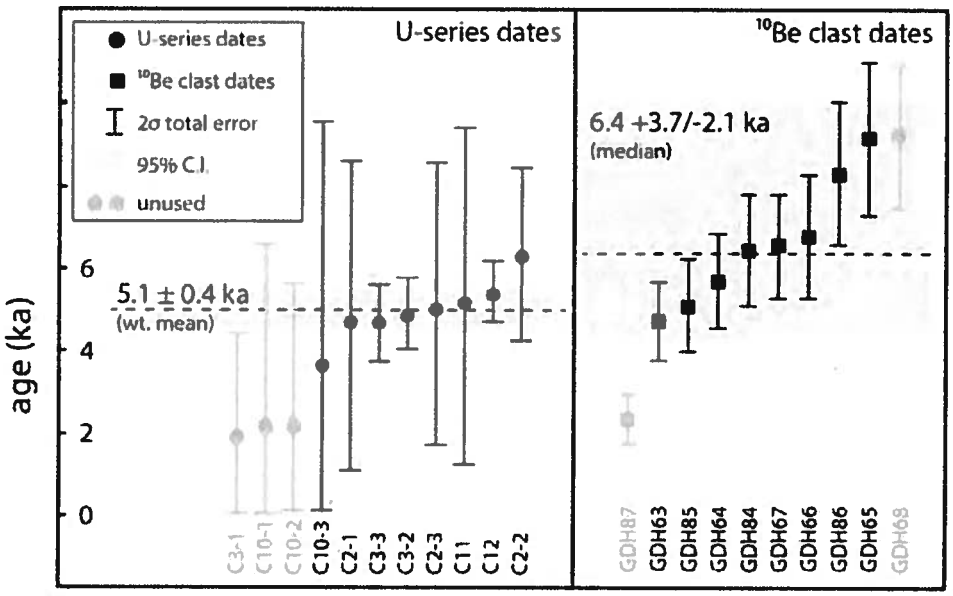

Figure 8 Results of U-series dating of pedogenic carbonate clast coatings from 5 pebbles (left), and ^{10}Be clast exposure dates for comparison (right). Individual measurements are shown with 2σ total errors, and show significant overlap between the distributions of measurements from both methods. Samples excluded from the weighted mean (U-series) and median (exposure dating) calculations are shown in grey. The mean U-series age and median clast exposure age overlap at the 95% confidence level. The mean U-series age provides a minimum depositional age for Qfr.

We determine the best-constrained Holocene right-lateral slip rate for the Banning strand of 3.9 +2.3/-1.6 mm/yr (median, 95% C.I.) by combining the 6.4 +3.7/-2.1 ka (95% C.I.) median combined surface clast age with the 25 ± 5 m, quantitatively determined fan axis offset. We also report a similar maximum slip rate of 4.9 +1.0/-0.9 mm/yr (median, 95% C.I.) by combining the 5.1 ± 0.4 ka U-series carbonate minimum age with the offset. The slip rate predicted by the 2.9 ± 0.7 ka (2σ) depth profile age is 8.6 +3.3/-2.3 mm/yr (median, 95% C.I.), although we are more confident in the U-series and clast exposure ages, so we do not favor this rate in our discussion of how these new slip rates affect our understanding of seismic hazard and slip partitioning in southern California.

5. Implications for earthquake hazard and slip partitioning

Our preferred Holocene right-lateral geologic slip rate for the Banning strand of 4-5 mm/yr represents only 25-35% of the right-lateral geologic slip rate for the southern Mission Creek strand (14-17 mm/yr) (Behr et al., 2010), and around 20% of the geodetically estimated slip rate for the Indio strand of the Coachella Valley segment of the southern San Andreas Fault (~23-25 mm/yr) (Becker et al., 2005; Fay and Humphreys, 2005; Fialko, 2006; Spinler et al., 2010; Loveless and Meade, 2011). This implies that only about 20-35% of total southern San Andreas Fault slip is transferred northwest into San Gorgonio Pass via the Banning strand.

The primary implication of this relatively low 4-5 mm/yr slip rate for the Banning strand is that slip may be more evenly distributed between the Banning, Garnet Hill, and Mission Creek strands in the northwestern Coachella Valley than was previously thought,

as illustrated in Figure 9a. A slip rate of 4-5 mm/yr, or 25-35% of geologically measured slip on the southern San Andreas Fault, is consistent with recent mechanical slip rate models (Fattaruso et al., 2014), but is significantly less than has been assumed in seismic hazard models and is inconsistent with it being a dominant structure transferring plate boundary slip to the northwest. This leaves 65-75% (~9-13 mm/yr) of southern San Andreas Fault slip to be taken up by the Mission Creek and/or Garnet Hill strands, or by faults that have not been identified. It is worth considering the possibility that southeast propagating ruptures could contribute to the offset of the Qfr fan without continuing far enough south to contribute offset to the Biskra Palms Oasis slip rate site. If this occurred relatively frequently, the slip rate we have measured would represent an even smaller proportion of southern San Andreas Fault slip. However, it remains unclear to what extent ruptures can actually propagate though San Gorgonio Pass, and given the abrupt northwest termination of the Banning strand and the lack of obvious connectivity between it and the San Gorgonio Pass Fault system, slip from southeast propagating ruptures is unlikely to have a significant affect on our slip rate measurement. Regardless, the model proposed in Figure 2a, whereby slip is concentrated on the Banning strand, appears to be invalid. Several slip-partitioning models are therefore possible, including that illustrated in Figure 9a, where slip is approximately evenly shared between the Mission Creek, Banning and Garnet Hill strands. A potential issue with this model is that the surface trace of the Mission Creek strand, although well expressed north of the Indio Hills, is not suggestive of a fault accommodating significant slip northwest of Desert Hot Springs (see Section 3.1, Fig. 3), and it does not displace Holocene alluvium higher in San Bernardino Mountains (Matti and Morton, 1993; Kendrick et al., 2015; Owen et al., 2014). This can be resolved to a certain extent by invoking northward slip transfer from the Mission Creek strand via faults in the Eastern Transverse Ranges (Fig. 1) to the Eastern California Shear Zone, which geologic slip rate measurements suggest accommodates 6.2 ± 1.9 mm/yr of right lateral slip over a 60 km wide shear zone (Oskin et al., 2008). Although the northern ends of the Burnt Mountain and Eureka Peak faults did rupture during the 1992 Landers earthquake, many of the Eastern Transverse Ranges faults are bedrock bounded, making assessments of late Quaternary activity difficult, and it is possible that slip transfer through this region may simply be too distributed to confidently quantify.

An alternative model that places less emphasis on the Mission Creek strand would place much of the slip not accommodated by the Banning strand on the Garnet Hill strand, making this the dominant fault in the northwestern Coachella Valley (Fig. 9b). Little is known about the Garnet Hill strand, partly because it is so poorly expressed at the surface. While folding and uplifts along the Garnet Hill strand seem to indicate a reverse slip component, the topography of Edom Hill to the south and the Whitewater Hills to the north may be related to complex interaction with the Banning strand, and it remains unclear exactly what relationship Garnet Hill (Fig. 1) has to latest Quaternary deformation along the Garnet Hill strand (Yule and Sieh, 2003). If this model (Fig. 9b) best represents present day slip partitioning, then coseismic slip associated with southern San Andreas Fault ruptures may tend to be partitioned between the Garnet Hill and Banning strands, with dominantly right lateral slip that is initially concentrated on the southeastern Banning strand transitioning to the northwest to right-reverse slip concentrated on the Garnet Hill strand as the strike of both faults rotates to a more

transpressive geometry near San Gorgonio Pass. While it is certainly possible that the Garnet Hill strand accommodates a significant lateral slip component as it enters San Gorgonio Pass (Yule and Sieh, 2003), this would be somewhat surprising given that there is little evidence along its surface trace, where identifiable, of offset consistent with a fault accommodating ~10 mm/yr.

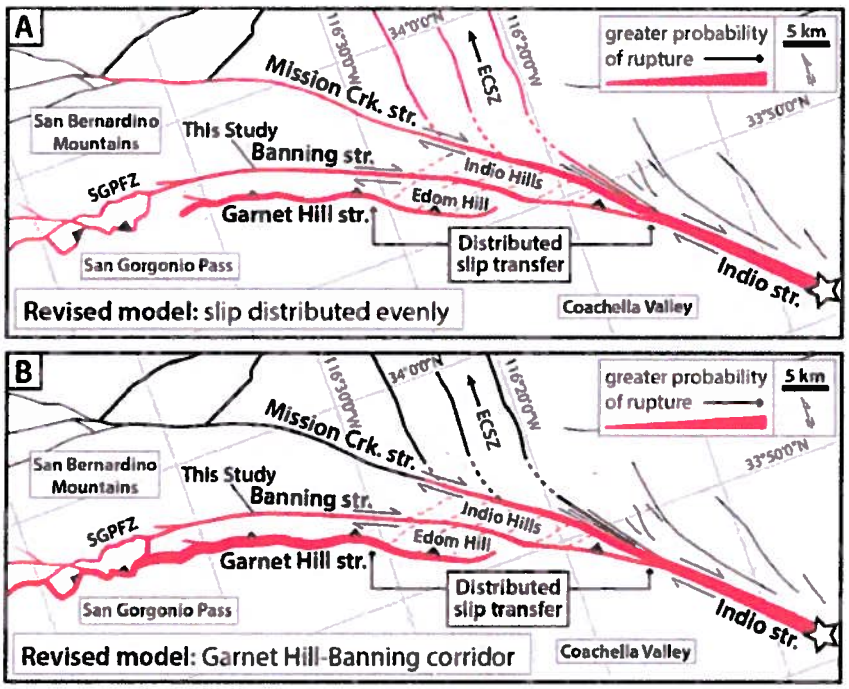

Figure 9 Revised models for how slip may be partitioned between the Mission Creek, Banning and Garnet Hill strands given the relatively low Banning strand slip rate. A) Slip is more evenly distributed between all three faults in the northwestern Coachella Valley. In this case, the majority of southern San Andreas Fault slip is still transferred northwest to San Gorgonio Pass via the Banning and Garnet Hill strands, with a smaller proportion transferred to the Eastern California Shear Zone via the Mission Creek strand. B) Slip is concentrated on the Garnet Hill strand and, to a lesser extent, the Banning strand. In this case, southern San Andreas Fault slip is almost entirely transferred northwest to San Gorgonio Pass.

This new slip rate for the Banning strand leads us to conclude that slip is not concentrated on the Banning strand, and may be more evenly partitioned between all three faults in the northwestern Coachella Valley or largely concentrated on the Garnet Hill strand. This result underscores the need for paleoseismic measurements of earthquake timing as well as additional slip rate measurements from all the major fault strands in order to adequately assess the hazard associated with northwest propagating earthquake ruptures.

6. Summary

The primary conclusions of this study are as follows.

1) Structural measurements and geomorphic observations suggest that slip is transferred from the Mission Creek strand to the Banning strand in the

northwestern Indio Hills, west of Thousand Palms Canyon.

2) The quantitatively constrained Holocene geologic slip rate for the Banning strand is 4-5 mm/yr since ~5.1-6.4 ka. This is a minimum slip rate for the Banning strand, since some slip may be transferred to the Garnet Hill strand before reaching the Painted Hill slip rate site.
3) 4-5 mm/yr of slip therefore enters San Gorgonio Pass. This is a minimum because the slip rate for the Garnet Hill strand is unknown.
4) 4-5 mm/yr represents only ~25-35% of the total amount of slip accommodated by the Coachella Valley segment of the San Andreas Fault, implying that slip is less concentrated on the Banning strand than previously thought.
5) The more prominent geomorphic expression of the trace of the Banning strand relative to the Garnet Hill and Mission Creek strands cannot be explained by a faster slip rate and may instead indicate more recent surface rupture or result from other factors favoring geomorphic preservation of the fault trace.
6) Although current seismic hazard models may not be incorrect in assuming that the next southern San Andreas Fault earthquake will rupture the Banning strand, they should consider other scenarios in which the Banning and Garnet Hill strands rupture together or are completely bypassed in favor of the Mission Creek strand or where all three faults rupture together.
7) Because our understanding of the geomorphic processes that contribute to the formation, stabilization and evolution of alluvial deposits is incomplete, use of multiple complimentary geochronometers may help to reduce the likelihood that erroneous depositional ages will be interpreted from dates that are incorrect because of unknown epistemic uncertainties.
8) Our results emphasize the urgent need to collect a greater number of slip rate measurements and paleoseismic constraints on earthquake timing from the Mission Creek, Banning and Garnet Hill strands in order to produce better informed hazard estimates for southern California, and to improve our understanding of the evolution of this fault system.

Resulting Publications

Gold, P.O., Behr, W.M., Rood, D., and Sharp, W.D., 2015, Holocene geologic slip rate for the Banning strand of the southern San Andreas Fault, southern California: Journal of Geophysical Research, doi: 10.1002/(ISSN)2169-9356.

(Accepted article online 21 July 2015).

References

Allen, C.R., 1957, San Andreas Fault zone in San Gorgonio Pass, Southern California: Geological Society of America Bulletin, v. 68, p. 315, doi: 10.1130/0016-7606(1957)68[315:SAFZIS]2.0.CO;2.

Becker, T.W., Hardebeck, J.L., and Anderson, G., 2005, Constraints on fault slip rates of the southern California plate boundary from GPS velocity and stress inversions: Geophysical Journal International, v. 160, p. 634–650, doi: 10.1111/j.1365-246X.2004.02528.x.

Behr, W.M., Rood, D.H., Fletcher, K.E., Guzman, N., Finkel, R., HANKS, T.C., Hudnut, K.W., Kendrick, K.J., Platt, J.P., Sharp, W.D., Weldon, R.J., and Yule, J.D., 2010, Uncertainties in slip-rate estimates for the Mission Creek strand of the southern San Andreas fault at Biskra Palms Oasis, southern California: Geological Society of America Bulletin, v. 122, p. 1360–1377, doi: 10.1130/B30020.1.

Dibblee, T.W., 2008, Geologic map of the Thousand Palms & Lost Horse Mountain 15 minute quadrangles, Riverside County, California. 1:62,500: Dibblee Foundation Map DF-372.

Fattaruso, L.A., Cooke, M.L., and Dorsey, R.J., 2014, Sensitivity of uplift patterns to dip of the San Andreas fault in the Coachella Valley, California: Geosphere, v. 10, p. 1235–1246, doi: 10.1130/GES01050.1.

Fay, N.P., and Humphreys, E.D., 2005, Fault slip rates, effects of elastic heterogeneity on geodetic data, and the strength of the lower crust in the Salton Trough region, southern California: Journal of Geophysical Research: Solid Earth (1978–2012), v. 110, doi: 10.1029/2004JB003548.

Fialko, Y., 2006, Interseismic strain accumulation and the earthquake potential on the southern San Andreas fault system: Nature, v. 441, p. 968–971, doi: 10.1038/nature04797.

Field, E.H., Arrowsmith, R.J., Biasi, G.P., Bird, P., Dawson, T.E., Felzer, K.R., Jackson, D.D., Johnson, K.M., Jordan, T.H., Madden, C., Michael, A.J., Milner, K.R., Page, M.T., Parsons, T., et al., 2014, Uniform California Earthquake Rupture Forecast, Version 3 (UCERF3)--The Time-Independent Model: Bulletin of the Seismological Society of America, v. 104, p. 1122–1180, doi: 10.1785/0120130164.

Field, E.H., Biasi, G.P., Bird, P., Dawson, T.E., Felzer, K.R., Jackson, D.D., Johnson, K.M., Jordan, T.H., Madden, C., Michael, A.J., Milner, K.R., Page, M.T., Parsons, T., Powers, P.M., et al., 2015, Long-Term Time-Dependent Probabilities for the Third Uniform California Earthquake Rupture Forecast (UCERF3): Bulletin of the Seismological Society of America, v. 105, p. 511–543, doi: 10.1785/0120140093.

Field, E.H., Dawson, T.E., Felzer, K.R., Frankel, A.D., Gupta, V., Jordan, T.H., Parsons, T., Petersen, M.D., Stein, R.S., Weldon, R.J., and Wills, C.J., 2009, Uniform California Earthquake Rupture Forecast, Version 2 (UCERF 2): Bulletin of the Seismological Society of America, v. 99, p. 2053–2107, doi: 10.1785/0120080049.

Fumal, T.E., Weldon, R.J., Biasi, G.P., Dawson, T.E., seitz, G.G., Frost, W.T., and Schwartz, D.P., 2002, Evidence for large earthquakes on the San Andreas fault at the Wrightwood, California, paleoseismic site: AD 500 to present: Bulletin of the

Seismological Society of America, v. 92, p. 2726–2760.

Gold, P.O., Behr, W.M., Rood, D., and Sharp, W.D., 2015, Holocene geologic slip rate for the Banning strand of the southern San Andreas Fault, southern California: Journal of Geophysical Research, doi: 10.1002/(ISSN)2169-9356.

Keller, E.A., Bonkowski, M.S., Korsch, R.J., and Shlemon, R.J., 1982, Tectonic geomorphology of the San Andreas fault zone in the southern Indio Hills, Coachella Valley, California: Geological Society of America Bulletin, v. 93, p. 46–56, doi: 10.1130/0016-7606(1982)93<46:TGOTSA>2.0.CO;2.

Kendrick, K.J., Matti, J.C., and Mahan, S.A., 2015, Late Quaternary slip history of the Mill Creek strand of the San Andreas fault in San Gorgonio Pass, southern California: The role of a subsidiary left-lateral fault in strand switching: Geological Society of America Bulletin,, p. 1–26, doi: 10.1130/B31101.1.

Loveless, J.P., and Meade, B.J., 2011, Stress modulation on the San Andreas fault by interseismic fault system interactions: Geology, v. 39, p. 1035–1038, doi: 10.1130/G32215.1.

Matti, J.C., and Morton, D.M., 1993, Paleogeographic evolution of the San Andreas fault in southern California: A reconstruction based on a new cross-fault correlation: The San Andreas fault system: Displacement, palinspastic reconstruction, and geologic evolution, v. 178, p. 107–159.

Matti, J.C., Morton, D.M., and Cox, B.F., 1992, The San Andreas fault system in the vicinity of the central Transverse Ranges province, southern California: v. 92.

Oskin, M., Perg, L., Shelef, E., Strane, M., Gurney, E., Singer, B., and Zhang, X., 2008, Elevated shear zone loading rate during an earthquake cluster in eastern California: Geology, v. 36, p. 507, doi: 10.1130/G24814A.1.

Owen, L.A., Clemmens, S.J., Finkel, R.C., and Gray, H., 2014, Quaternary Science Reviews: Quaternary Science Reviews, v. 87, p. 114–134, doi: 10.1016/j.quascirev.2014.01.003.

Philibosian, B., Fumal, T., and Weldon, R., 2011, San Andreas Fault Earthquake Chronology and Lake Cahuilla History at Coachella, California: Bulletin of the Seismological Society of America, v. 101, p. 13–38, doi: 10.1785/0120100050.

Sieh, K.E., 1994, Late Quaternary slip rate of the north branch of the San Andreas fault at City Creek, California: Geological Society of America Abstracts with Programs 2, 91 p.

Spinler, J.C., Bennett, R.A., Anderson, M.L., McGill, S.F., Hreinsdóttir, S., and McCallister, A., 2010, Present-day strain accumulation and slip rates associated with southern San Andreas and eastern California shear zone faults: Journal of Geophysical Research, v. 115, p. B11407, doi: 10.1029/2010JB007424.

Van der Woerd, J., Klinger, Y., Sieh, K., Tapponnier, P., Ryerson, F.J., and Mériaux, A.-S., 2006, Long-term slip rate of the southern San Andreas Fault from 10Be- 26Al surface exposure dating of an offset alluvial fan: Journal of Geophysical Research, v. 111, p. B04407, doi: 10.1029/2004JB003559.

Weldon, R.J., Fumal, T.E., Biasi, G.P., and Scharer, K.M., 2005, Past and future earthquakes on the San Andreas fault: Science, v. 308, p. 966–967.

Weldon, R.J., II, 2010, Slip rate for the North Branch of the San Andreas fault, San Bernardino Valley: Southern California Earthquake Center Annual Report,, p. 1–5.

Yule, D., and Sieh, K., 2003, Complexities of the San Andreas fault near San Gorgonio Pass: Implications for large earthquakes: Journal of Geophysical Research: Solid Earth (1978–2012), v. 108, doi: 10.1029/2001JB000451.

Zechar, J.D., and Frankel, K.L., 2009, Incorporating and reporting uncertainties in fault slip rates: Journal of Geophysical Research, v. 114, p. B12407, doi: 10.1029/2009JB006325.